https://dx.doi.org/10.21577/0103-5053.20220041

J. Braz. Chem. Soc., Vol. 33, No. 10, 1211-1218, 2022

Article

Evaluation of the Structural Integrity of Layered Double Hydroxides and Mesoporous Silica During the Preparation of Heterostructures

Lister P. Bianconi,[a,b] *Christine Taviot-Gueho,*[c] *Vera Regina L. Constantino*[b] *and Marcos Augusto Bizeto*[*,a]

[a]*Departamento de Química, Instituto de Ciências Ambientais, Químicas e Farmacêuticas, Universidade Federal de São Paulo, 09913-030 Diadema-SP, Brazil*

[b]*Departamento de Química Fundamental, Instituto de Química, Universidade de São Paulo, 05508-900 São Paulo-SP, Brazil*

[c]*Institut de Chimie de Clermont-Ferrand (ICCF), SIGMA Clermont, CNRS, Université Clermont Auvergne, F-63000 Clermont-Ferrand, France*

Heterostructures constructed with mesoporous silica and layered double hydroxides are interesting for catalytic and drug delivery applications. Different arrangements between these phases are possible. In this study, we prepared heterostructures by embedding layered double hydroxides phases $[M_4Al_2(OH)_{12}](CO_3)$ (M = Mg^{2+} or Zn^{2+}) within the MCM41 mesoporous silica type phase. According to our results, the most critical step of this preparation is the removal of the organic template used to create the mesopores in the silica phase, which can be done by calcination or extraction with solvent, normally a mixture of ethanol and a mineral acid. The results reported in this study demonstrate that both can cause structural changes in the components of the heterostructure at different extensions. Calcination promoted the collapse of the layered hydroxide phases. Attempts made for their reconstruction through rehydration, which is a quite known process, were not completely effective and also dependent on the chemical composition of the layered phase. The complete template removal with preservation of the layered phases was possible using the extraction method but by replacing the mineral acid with NH_4Cl. However, some discrete structural changes were identified possibly due to a partial lixiviation of Al^{3+} from the double hydroxide layers.

Keywords: layered double hydroxide, mesoporous silica, MCM41, heterostructures

Introduction

The first study about a heterostructure prepared by combining mesoporous silica (MS) with layered double hydroxide (LDH) was reported in 2008.[1] This material was produced with the intention of improving the catalytic activity of the magnesium-aluminum LDH (Mg_4Al_2-LDH) by restricting the lateral growth of the hydroxide particles by preparing them directly inside the mesopores of the SBA15 silica. These heterostructures can also be prepared by depositing exfoliated LDH layers onto the surface of the MS particles. The heterostructures with such arrangement were already evaluated as drug carriers,[2-4] flame retardant additive for polymers,[5] pollutant absorbers[6] and catalyst.[7]

A third possible arrangement for such heterostructures comprises the LDH particles embedded within the MS phase. This approach was concomitantly reported by Liu *et al.*[8] and Bao *et al.*[9] to obtain drug carriers. More recently, Harrison *et al.*[10] evaluated the influence of the thickness of the MS outer layer and the diameter of the mesopores in the release of folic acid that was previously intercalated into the Mg_4Al_2-LDH. Cao *et al.*[11] produced a core-shell type heterostructure with an ultrathin outer layer of MS and evaluated the *in vivo* and *in vitro* release of curcumin, previously intercalated into the LDH core. Little attention was devoted to understanding the influence of the synthetic conditions on the structural integrity and organization of the phases in such heterostructure.

One of the critical steps in the preparation of heterostructures containing the layered phase embedded within the mesoporous silica matrix is the template removal

*e-mail: mabizeto@unifesp.br
Editor handled this article: Humberto O. Stumpf (Associate)

from the pores of silica counterpart. The mesopores of the silica phase can be produced using organic templates, composed of micellar aggregates of ionic or non-ionic surfactants,[12] which must be removed from the material to allow accessibility and diffusion within the created pores. This removal can be done with calcination or extraction using a mixture of ethanol and mineral acid. However, these processes can be potentially detrimental to the structural integrity of the layered double hydroxide phase. Thus, in this study, we synthesized heterostructures of the layered double hydroxide phases $[M_4Al_2(OH)_{12}](CO_3)$ (M = Mg^{2+} or Zn^{2+}) embedded within a matrix of the mesoporous silica MCM41 and evaluated the impact of these template removal processes on the structural integrity of the components of the heterostructure and on the porosity of the material.

Experimental

$MgCl_2{\cdot}6H_2O$, $AlCl_3{\cdot}6H_2O$, $ZnCl_2$, Na_2CO_3, NaOH, cetyltrimethylammonium bromide (CTAB), tetraethylorthosilicate (TEOS), and trimethylchlorosilane (TMCS) were supplied by Sigma-Aldrich (Darmstadt, Germany). Ammonia solution (27%), ethanol (95%), toluene, and NH_4Cl were provided by LabSynth (São Paulo, Brazil). All reagents were used as received.

Synthesis of LDH

LDH with compositions $[M_4Al_2(OH)_{12}]CO_3.nH_2O$, where M = Mg^{2+} or Zn^{2+} were prepared using the co-precipitation method at pH value 9.0. In a typical synthesis made at room temperature, 150 mL of the solution of cations containing 4.1 g (0.02 mol) of $MgCl_2.6H_2O$ and 2.4 g (0.01 mol) of $AlCl_3.6H_2O$ (or 2.8 g $ZnCl_2$-0.02 mol) and 2.4 g (0.01 mol) of $AlCl_3.6H_2O$ and 150 mL of a 0.4 mol L^{-1} solution containing Na_2CO_3 and NaOH were dropped under stirring at 900 rpm into 200 mL of deionized water (ultrapure Milli-Q water) using an automatic titrator to maintain the pH of the mixture constant at 9.0. After the complete addition of the solutions, the mixture was heated to 55 °C and maintained under continuous stirring during 16 h to promote the aging of the LDH's particles. Then the solid was centrifuged and washed with water until the complete removal of the chloride ions, which was confirmed by adding drops of an $AgNO_3$ solution to a sample of the supernatant. Finally, the LDH samples were ultrasonically dispersed in deionized water, frozen in liquid nitrogen and freeze-dried. The isolated LDH samples, hereafter identified in the text as Mg_4Al_2-LDH or Zn_4Al_2-LDH, were characterized by X-ray diffractometry (XRD), Fourier-transformed infrared vibrational spectroscopy (FTIR) and scanning electron microscopy (SEM). The porosity of the materials was measured by N_2 physisorption isotherms. The metal amounts in the LDH were determined by inductively coupled plasma optical emission spectroscopy (ICP-OES) while the water amount was determined by thermogravimetric analysis (TGA). The calculated chemical composition of the synthesized LDH were $[Mg_{4.2}Al_2(OH)_{12.4}](CO_3){\cdot}4.8H_2O$ and $[Zn_{4.4}Al_2(OH)_{12.8}](CO_3){\cdot}7.0H_2O$.

Synthesis of heterostructures

The whole synthetic process of the heterostructures is schematically illustrated in Figure 1. In a typical synthesis, 200 mg of a LDH lyophilized sample ($[Mg_{4.2}Al_2(OH)_{12.4}](CO_3){\cdot}4.8H_2O$ or $[Zn_{4.4}Al_2(OH)_{12.8}](CO_3){\cdot}7.0H_2O$) was ultrasonically dispersed in 15 mL of deionized water; then 0.09 g of CTAB was dissolved in 5.2 mL of an NH_3 solution (27%). This mixture was kept under constant stirring at room temperature for about 30 min and then 0.4 mL of TEOS was dropped under continuous stirring and allowed to react at room temperature for 6 h. The final molar ratios among the reactants were: 0.5 LDH : 1TEOS : 0.1 CTAB : 68 NH_3 : 526 H_2O. The resultant solid was centrifuged, washed with water, dried at 60 °C in a reduced pressure drying oven for 24 h, and then characterized by XRD and FTIR techniques. This synthetic procedure was carried out for both LDH phases and each of the isolated solid samples will be abbreviated as M_4Al_2@MCM41, where M = Mg or Zn. Afterward, these samples were divided into two fractions (Figure 1). One fraction was modified with TMCS and then calcined to remove the template from the silica pores. The other fraction was submitted to the template removal by extraction with an ethanol/NH_4Cl solution.

According to Bao *et al.*,[9] the post-grafting of TMCS on the silica surface avoids the agglomeration of the particles upon calcination, and the process was made in dry toluene solution (50 mL) containing 0.06 mL of silane under reflux for 24 h. This sample was then calcined at 550 °C in a tubular furnace using a heating rate of 2 °C min^{-1} under N_2 flow upon reaching the desired temperature; then the N_2 flow was changed to air with the adjusted temperature maintained for 6 h. The calcination was repeated twice in airflow to ensure the complete removal of any residual charred material. The heterostructures produced by calcination will be identified hereafter as $M_4Al_2@MCM41_{calc}$ (M = Mg^{2+} or Zn^{2+}). After calcination, the samples were rehydrated in 1 mol L^{-1} bicarbonate solution along 72 h to promote the reconstruction of the

LDH core. The hydrated heterostructures will be identified from now as M_4Al_2@MCM41$_{calc\text{-}hyd}$ (M = Mg^{2+} or Zn^{2+}).

The other solid fraction was submitted to the template extraction process carried out dispersing 300 mg of the prepared heterostructure still containing CTA^+ into the pores in 20 mL of a solution containing 0.4 g of NH_4Cl in ethanol (Figure 1). This dispersion was kept refluxing under stirring for 40 h. The progression of the template removal was monitored by FTIR analysis of samples collected at different time intervals. When the CTA^+ presence in the material was no more detected by FTIR, the solid was washed with ethanol and dried at 60 ºC in a reduced pressure drying oven. The samples obtained by the extraction of the organic template from the silica pores will be identified as M_4Al_2@MCM41$_{ext}$ (M = Mg^{2+} or Zn^{2+}). The characterization of all these heterostructures was carried out by XRD, FTIR, SEM, transmission electron microscopy (TEM) and isotherms of N_2-physisorption.

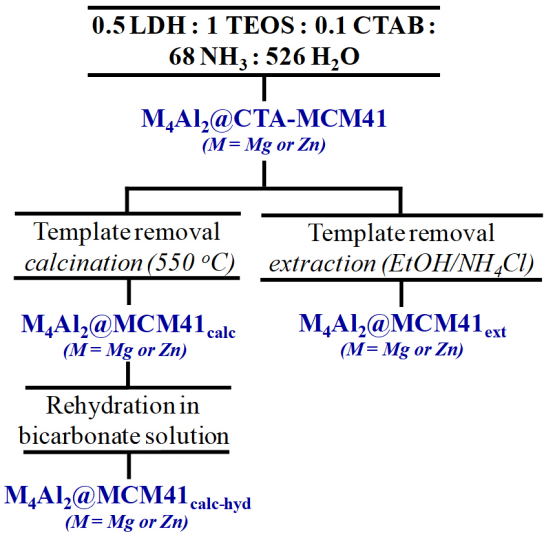

Figure 1. Scheme of the synthetic steps for the preparation of the LDH@MS heterostructures.

Characterization techniques

X-ray diffraction patterns (XRD) of powdered samples were registered in a Rigaku (Tokyo, Japan) diffractometer, model Miniflex, using Cu Kα radiation (1.541 Å, 30 kV, and 15 mA). N_2 physisorption isotherms were registered at 77 K in an ASAP 2020N Automatic Physisorption Analyzer from Micromeritics (Atlanta, USA). Samples were degassed at 80 ºC for 48 h before analysis. Scanning electron microscopy (SEM) images were registered in a JEOL (Tokyo, Japan) microscope, model JSM-6610LV, using the SEI detector. Powdered samples were deposited on a carbon tape and then coated with gold using a Desk V cold sputter/etch unit. Transmission electron microscopy (TEM) images were recorded in a JEOL (Tokyo, Japan) microscope, model JEM 2100, operating at 200 kV and equipped with an energy-dispersive X-ray spectroscopy (EDS) from Oxford Instruments. Samples were prepared by ultrasonically dispersing the heterostructures in isopropanol followed by deposition onto a carbon-coated Cu microgrid. Fourier transformed infrared (FTIR) spectra were recorded in a Shimadzu (Kyoto, Japan) spectrophotometer, model IRPrestige 21, using the diffuse reflectance mode, the DRIFT accessory, and 4 cm^{-1} of resolution and 264 scans.

Structural refinement

The Le Bail method[13] comprising the full-pattern decomposition of the XRD pattern of the powdered sample was used to determine the cell parameters of LDH assuming the typical R-3m space group. The profiles refinements were carried out using the FullProf suit package.[14] A linear combination of spherical harmonics was used to model peak broadening and allowing the calculation of the volume-averaged apparent size of the crystallites in the direction normal to the scattering planes. LaB_6 NIST standard was used to take into account the instrumental effect.

Results and Discussion

As already reported in the introduction, little attention was devoted in the already published papers on the understanding of the influence of adopted synthetic conditions and procedures on the structure of the component phases of the heterostructure. The thermal treatment used to remove the organics used as the template of the mesopores of the silica phase can be especially detrimental. Thus, in this study we made the synthesis of heterostructures using low amounts of the surfactant cetyltrimethylammonium bromide necessary to produce the mesopores in the silica phase. We evaluated if the modifications made in the synthetic procedure can facilitated the process of template removal and can influenced the porosity of the formed heterostructures.

The arrangement between LDH and MS phases in the heterostructures was first examined by scanning and transmission electron microscopies. The SEM images of the lyophilized LDH precursors (Figures 2a and 2e) showed the presence of platelet aggregated particles known as "sand rose". With the deposition of the silica matrix, the initial LDH "sand-rose" aggregation was not ever observed (Figures 2b and 2f), suggesting that the MS phase was formed around them. For comparison purposes, the SEM images of heterostructures synthesized as reported in the literature[9] were also registered. Such images (see Figure S1

in Supplementary Information (SI) section) showed the presence of particles with two different shapes: one similar to the LDH particles and a spherical one, suggesting the presence of segregated phases. Spherical mesoporous silica particles are formed when of ammonia and ethanol are present in the reaction medium,[15] as like in the synthetic procedure we followed from the literature that used a molar ratio among the reactants of 1 TEOS : 0.9 CTAB : 820 NH_3 : 1050 EtOH : 4680 H_2O.[9] Thus, one of the impacts of the 89% of reduction in the molar amount of CTAB without the usage of ethanol in the reaction medium was to avoid the formation of these segregate phases. Spherical particles were not observed in the SEM images (Figures 2b and 2f). The registered TEM images revealed that these particles are formed by aggregates containing the LDH particles embedded into the silica phase, which has the mesopores easily observed in the images (Figures 2c and 2g). The EDS elemental analysis (Figures 2d and 2h) confirmed the presence of LDH in the solid. A detailed visualization of one LDH particle was possible using higher magnification, as shown in the inset of Figure 2c. The regularly-spaced dark fringes represent the layers stacking of an LDH particle. The space measured between these fringes was 7.6 Å, which is equivalent to the (003) stacking planes that also appeared as a diffraction peak in Figure 3a. The high intensity of the electron beam required to observe the LDH particle in detail caused the mesostructure collapse of the silica phase in the surrounding.

The XRD patterns of starting LDHs (Figures 3a and 3e) showed the Zn_4Al_2-LDH more crystalline than the Mg_4Al_2-LDH, as already reported in literature.[16] With the formation of the heterostructures, the diffractograms registered before the template removal (Figures 3a and 3b) showed peaks identified with asterisks at the low angle region attributed to the silica mesophase and peaks at higher angles ascribed to the LDH phase.

The process of template removal using the EtOH/NH_4Cl solution was monitored with vibrational spectroscopy by periodically collecting samples of the solid from the suspension and registering their FTIR spectra. CTA^+ has characteristic high intensity vibrational bands at around 2925 and 2850 cm^{-1}, assigned to C–H stretching modes, and a less noticeable band at 1210 cm^{-1}, attributed to C–N stretching (see Figure S2 in SI section). When these bands disappeared completely, the extraction process was finished. Changes in the diffraction profiles were noticed after removing the template (Figures 3b and 3f). The intensity of all diffraction peaks decreased and the (100) peak attributed to the mesoporous ordering of the silica phase became undefined.

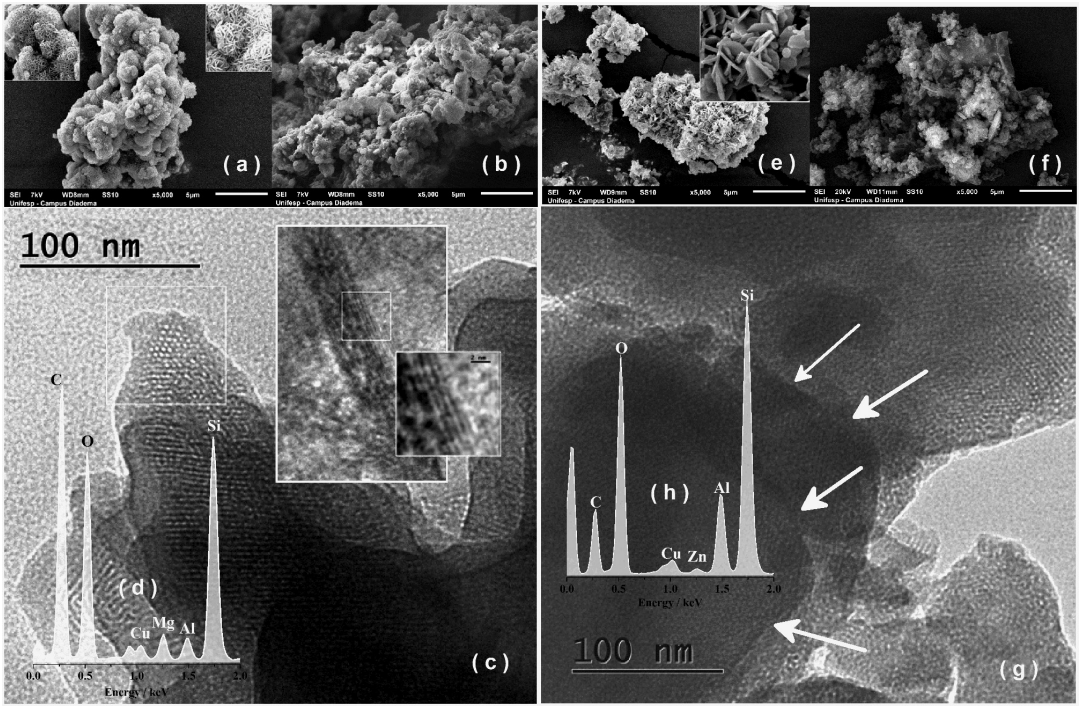

Figure 2. SEM images of (a) $[Mg_{4.2}Al_2(OH)_{12.4}](CO_3)\cdot 4.8H_2O$, (b) Mg_4Al_2@CTA-MCM41. The insets in (a) show magnified regions of the lyophilized LDH sample with a detailed view of the "sand-rose" aggregates. The scale bar in SEM images is 5 μm. (c) TEM image of the Mg_4Al_2@$MCM41_{ext}$ and the highlighted areas show the mesopores ordering of the outer silica layer in a perpendicular arrangement to the LDH particle and the detailed view of the layers stacking of the $[Mg_{4.2}Al_2(OH)_{12.4}](CO_3)$ particle embedded in the silica phase. (d) EDS elemental analysis of the aggregates shown in the TEM image. SEM images of (e) $[Zn_{4.2}Al_2(OH)_{12.4}](CO_3)\cdot 4.8H_2O$, (f) Zn_4Al_2@CTA-MCM41. The inset in (e) shows magnified region of the lyophilized LDH sample with the view of "sand-rose" aggregates. (g) TEM image of the Zn_4Al_2@$MCM41_{ext}$ and (h) EDS elemental analysis of the TEM image.

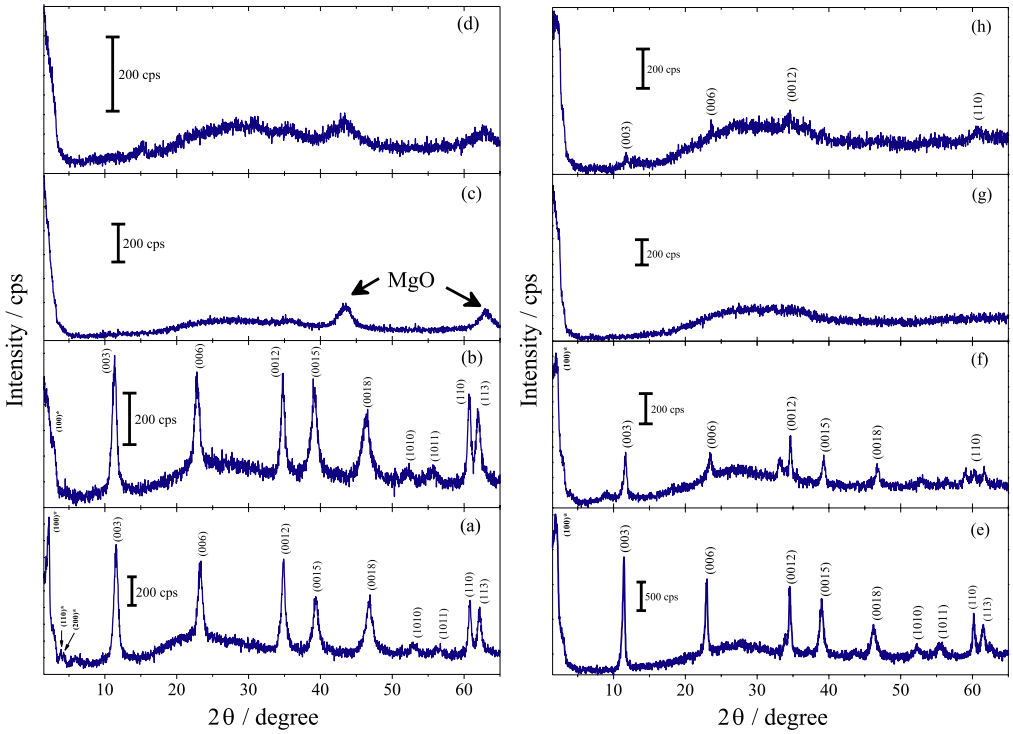

Figure 3. (left) XRD patterns of the Mg_4Al_2@MS heterostructures and (right) of the Zn_4Al_2@MS heterostructures. As-synthesized with the template inside the pores (a) Mg_4Al_2@CTA-MCM41 and (e) Zn_4Al_2@CTA-MCM41. The peaks identified with asterisks are referred to the silica mesophase and the peaks of LDH were indexed assuming a $3R_1$ polytype; after template removal by extraction with EtOH/NH_4Cl (b) Mg_4Al_2@$MCM41_{ext}$ and (f) Zn_4Al_2@$MCM41_{ext}$; after calcination at 550 ºC (c) Mg_4Al_2@$MCM41_{calc}$ and (g) Zn_4Al_2@$MCM41_{calc}$; after rehydration in bicarbonate solution for 72 h to reconstructed the LDH structure after calcination (d) Mg_4Al_2@$MCM41_{calc\text{-}hyd}$ and (h) Zn_4Al_2@$MCM41_{calc\text{-}hyd}$.

When the template was removed by calcination, the temperature required to accomplish it (550 ºC) was high enough to cause the collapse of the layered arrangement. The high temperature promotes the dehydroxylation of LDH layers and the decomposition of the interlayer carbonate anion, with the respective formation of metal oxide phases.[17,18] The FTIR spectra of the calcined solids (see Figure S2 in SI section) confirmed the absence of carbonate ions since the bands referred to this ion were not present in the registered spectra as also the bands referred to M–OH vibrations of LDH. The formation of a crystalline MgO phase was identified as a product of the thermal decomposition of the LDH phase in the Mg_4Al_2-LDH heterostructure (Figure 3c). In the case of the thermal decomposition of the LDH in the Zn_4Al_2-LDH heterostructure, the formation of crystalline phases was not observed (Figure 3g) indicating that only amorphous phases were formed in this process.

Calcination usually improves the mesostructural ordering of the mesoporous silica due to the formation of siloxane bonds among the structural [SiO_4] tetrahedral units, which results in well defined and intense diffraction peaks. However, in the case of the heterostructures with LDH, a decrease in the mesostructural ordering was observed after the thermal treatment. The (100) diffraction peak became undefined, which might be related to the products of the thermal decomposition possibly occupying or occluding the mesopores of the silica phase.

The layered structure of the LDH can be reconstructed from the mixture of decomposed metal oxides upon rehydration.[18] Hence, the possibility of using this approach was investigated for the first time in this study to a heterostructure. Thus, the rehydration of the thermally treated solids was carried out in a bicarbonate solution for 72 h. Diffraction peaks ascribed to the layered phases reappeared only to the heterostructure produced with the Zn_4Al_2-LDH (Figure 3h), but the peaks show low intensity when compared to diffraction profile of the LDH in the heterostructure before the calcination (Figure 3e).

A full pattern refinement of the XRD data was made to quantify the changes that occurred in the crystallites of the LDH phase present in the heterostructures (Figure 4). The unit cell parameters were first determined and they are related to the M^{2+}/M^{3+} molar ratio within LDH hydroxide layers.[19] Besides, the size of the coherent domains was estimated from the refined coefficients of the spherical harmonics model used. Due to the platelet shape of LDH crystals, the dimensions along the (110) and (00l) directions are assimilated to the in-plane dimension $L_{(110)}$ and the thickness $L_{(00l)}$ of the crystallites (Table 1). For instance, the

estimated lateral size of the Mg_4Al_2-LDH crystallites was compatible to the thickness of the particle observed in the TEM image shown as an inset in Figure 2c. In the pristine heterostructures (before template extraction) the refined data (Table 1) indicated the formation of LDH structures with cell parameters consistent with a M^{2+}/Al^{3+} ratio close to 2.8.

The template extraction did not affect the M^{2+}/Al^{3+} ratio of the LDH layer, but in the case of the heterostructure containing Zn_4Al_2-LDH, the size of coherent domains of the crystallites reduced when compared to the initial LDH (Table 1). The presence of diffraction peaks at 2θ = 27°, 29° and 58.5° indicates the presence of a mixture of $ZnO_2/Zn(OH)_2$,[20] which might be related to the disassembling of the layers by Al^{3+} lixiviation.

The reconstruction of the LDH phase after the rehydration in HCO_3^- solution was partially effective for the Zn_4Al_2-LDH heterostructure. The reconstructed crystallites had coherent domains with sizes of about half the size of the initial LDH, which were responsible for the low intensity of the diffraction peaks observed in X-ray diffractogram (Figure 4f). The achievement of a partial reconstruction for this LDH phase could be related to the time spent in hydration did not having been long enough. Another possibility is the formation of a phase resultant from the reaction between the silica and LDH promoted by the thermal treatment, which precludes the reconstruction of the layered phase. The absence of any diffraction peak that indicates the structural reconstruction of the Mg_4Al_2-LDH phase after rehydration of the calcined heterostructure, beyond the possibilities already described before, the formation of a stable crystalline MgO phase, as demonstrated in the diffractogram shown in Figure 3c, can also have contributed to unable the lamellar phase reconstruction. Thus, the use of calcination to remove the template molecules from SiO_2 in the heterostructure with LDH is not recommended, and so, the following characterization data will be referred only to the heterostructures where the template was removed by extraction.

The porosity of those heterostructures after the template removal by extraction was determined by analyzing the isotherms curves of the N_2 physisorption shown in Figure S3 in SI section. These isotherms can be classified as type IVa, as expected to mesoporous solids,[21] and the presence of a step-down in the desorption branch at the P/P_0 around 0.45 is related to porous structures with partially blocked mesopores.[21] A remarkable increase in the porosity and surface area of the heterostructure produced with the Zn_4Al_2-LDH was observed after template extraction (Table 2). The analysis of the C parameter of the Brunauer-Emmett-Teller (BET) equation is a way to confirm the validity of the surface area measurement and also to estimate the presence of micropores in the mesoporous matrix.[22]

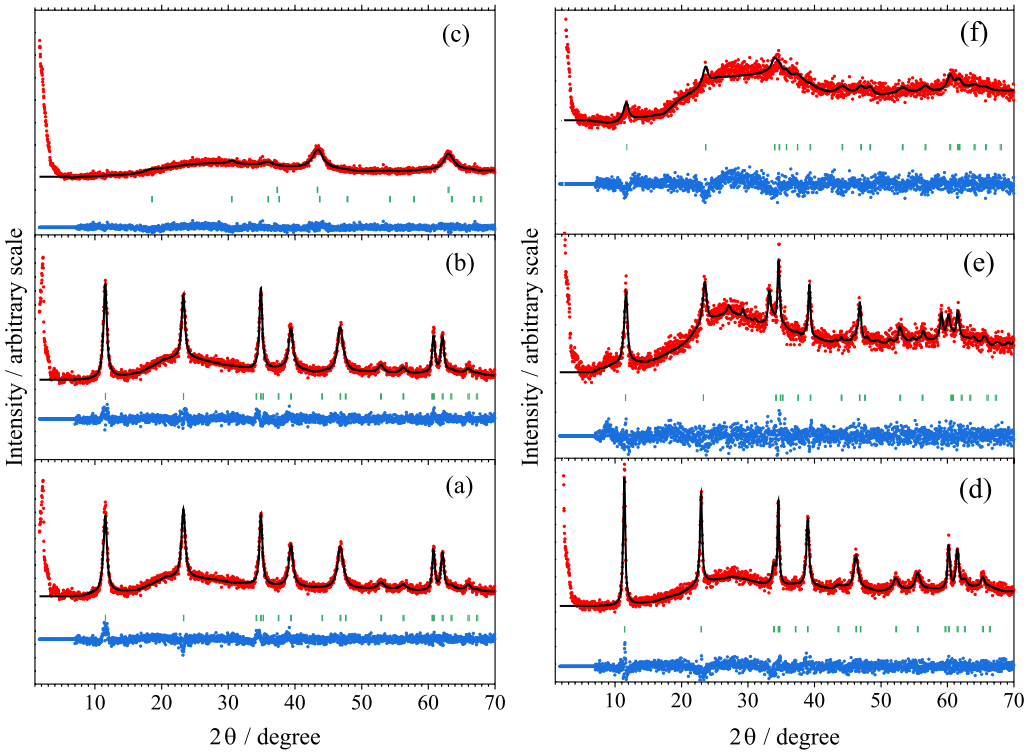

Figure 4. The full XRD patterns refinement of the LDH phase in (a) Mg_4Al_2@CTA-MCM41, (b) Mg_4Al_2@MCM41$_{ext}$, and (c) Mg_4Al_2@MCM41$_{calc\text{-}hyd}$. The full XRD patterns refinement of the LDH phase in (d) Zn_4Al_2@CTA-MCM41, (e) Zn_4Al_2@MCM41$_{ext}$, and (f) Zn_4Al_2@MCM41$_{calc\text{-}hyd}$. Experimental XRD pattern (red cross), calculated pattern (solid black line), difference profiles (solid blue line), and Bragg reflections (green ticks).

Table 1. Cell parameters (R-3m space group) and dimensions of LDH platelets obtained from the profile refinement of XRD data of heterostructures

Heterostructure	Crystalline phase	Cell parameters / Å	Size of LDH crystallites thickness $L_{(001)}$/in-plane $L_{(110)}$ / Å	M^{2+}/Al^{3+} ratio
Mg_4Al_2@CTA-MCM41	LDH	a = 3.047(1) c = 22.924(3)	90/185	2.8
Mg_4Al_2@MCM41$_{ext}$	LDH	a = 3.0478(1) c = 22.936(3)	100/175	2.8
Mg_4Al_2@MCM41$_{calc\text{-}hyd}$	LDH not detected			
Zn_4Al_2@CTA-MCM41	LDH	a = 3.0747(1) c = 23.241(3)	170/220	2.8
Zn_4Al_2@MCM41$_{ext}$	LDH	a = 3.07470 c = 22.660(4)	100/175	2.8
	$Zn(OH)_2$	Imm2 a = 23.07lb = 8.04 c = 3.30		
Zn_4Al_2@MCM41$_{calc\text{-}hyd}$	LDH	a = 3.065(1) c = 22.58(1)	65/70	2.2

LDH: layered double hydroxides.

As this parameter is related to the energy of monolayer adsorption, it acquires high values when a gas monolayer is formed in a microporous environment.[21] If C value is lower than 50 a monolayer overlaps with a multilayer bringing an imprecision to the value of the calculated surface area. When C value is lower than 2, the BET method is not applicable.[21] The C value of the pristine LDH phases reduced after the MS deposition (Table 2) due to the formation of the mesopores, which also promoted an increasing of the surface area. However, the C parameter of the BET equation decreased to around 60 in Zn_4Al_2@MCM41$_{ext}$, a value expected for solids containing ordered mesoporosity, which indicated that the pores in this heterostructure was more accessible than in Mg_4Al_2@MCM41$_{ext}$. Thus, the mixture of EtOH/NH_4Cl used to remove the template possibly promoted a lixiviation of the Mg_4Al_2-LDH and the products of this process seem to have deposited in the mesopores. The same effect was not observed to the Zn_4Al_2-LDH, suggesting that this material is resistant to the lixiviation.

Conclusions

In this study, we evaluated the influence of the chemical composition of the layered double hydroxides on the structural stability and porosity of heterostructures produced with the LDH phases embedded within mesoporous silica. We also made modifications in the synthetic procedure, related to the decrease in the amount of CTAB without using ethanol as co-solvent that avoided the formation of segregated phases as observed in the procedure reported in the literature. The most critical step was the removal of the template used to create the mesoporosity in the silica phase. Calcination led to the collapse and thermal degradation of the LDH phase. The attempts made to reconstruct the layered arrangement by rehydration were partially effective only to the Zn_4Al_2-LDH phase. The Mg_4Al_2-LDH phase was also sensitive to the removal of the template using a mixture of ethanol and NH_4Cl, as the resultant heterostructure showed a decrease in the available volume of pores, which we believe to be related to the deposition of the products from the lixiviation of the LDH particles inside the mesopores. In our data, the Zn_4Al_2-LDH phase was more adequate than Mg_4Al_2-LDH to construct the heterostructures. Synthetic efforts are still necessary to provide better control of the structural organization between the inorganic phases that constitute the heterostructure.

Table 2. Porosity data of the pristine LDH and the heterostructures with empty pores after template removal with EtOH/NH_4Cl

Material	C parameter	Specific surface area / (m^2 g^{-1})	Pore volume / (cm^3 g^{-1})
$[Mg_{4.2}Al_2(OH)_{12.4}](CO_3)$	173	104	0.68
Mg_4Al_2@MCM41$_{ext}$	117	217	0.34
$[Zn_{4.2}Al_2(OH)_{12.8}](CO_3)$	246	16	0.23
Zn_4Al_2@MCM41$_{ext}$	62	378	0.51

Supplementary Information

Supplementary data (SEM images, FTIR spectra and N_2 physisorption isotherms) are available free of charge at http://jbcs.sbq.org.br as PDF file.

Acknowledgments

Authors are thankful to Núcleo de Instrumentação para Pesquisa e Ensino (NIPE) do Centro de Equipamentos e Serviços Multiusuários (CESM-ICAQF, UNIFESP) for the SEM images recording. M.A.B. is thankful to the financial support from FAPESP (grant 2019/05467-0). L.P.B. is thankful to the fellowship from Coordenação de Aperfeiçoamento de Pessoal de Nível Superior - Brasil (CAPES) - Finance Code 001. V.R.L.C. is grateful to the Conselho Nacional de Desenvolvimento Científico e Tecnológico (CNPq) for the research grant (process 305446/2017-7). This work is part of the Research Academic Cooperation Agreement PRC-CNRS-FAPESP (PRC-Projets de recherché conjoints 1688 and SPRINT-São Paulo Researchers in International Collaboration 2016/50317-9).

References

1. Li, L.; Shi, J.; *Chem. Commun.* **2008**, 996.
2. Zheng, Q.; Hao, Y.; Ye, P.; Guo, L.; Wu, H.; Guo, Q.; Jiang, J.; Fu, F.; Chen, G.; *J. Mater. Chem. B* **2013**, *1*, 1644.
3. Jin, L.; Huang, Q. J.; Zeng, H. Y.; Du, J. Z.; Xu, S.; Chen, C. R.; *Microporous Mesoporous Mater.* **2019**, *274*, 304.
4. Wen, J.; Yang, K.; Ding, X.; Li, H.; Xu, Y.; Liu, F.; Sun, S.; *Inorg. Chem.* **2019**, *58*, 2987.
5. Jiang, S.-D.; Bai, Z.-M.; Tang, G.; Song, L.; Stec, A. A.; Hull, T. R.; Hu, Y.; Hu, W.-Z.; *ACS Appl. Mater. Interfaces* **2014**, *6*, 14076.
6. Jiang, S.-D.; Song, L.; Zeng, W.-R.; Huang, Z.-Q.; Zhan, J.; Stec, A. A.; Hull, T. R.; Hu, Y.; Hu, W.-Z.; *ACS Appl. Mater. Interfaces* **2015**, *7*, 8506.
7. Suo, H.; Duan, H.; Chen, C.; Buffet, J.-C.; O'Hare, D.; *RSC Adv.* **2019**, *9*, 3749.
8. Liu, J.; Harrison, R.; Zhou, J. Z.; Liu, T. T.; Yu, C.; Lu, G. Q.; Qiao, S. Z.; Xu, Z. P.; *J. Mater. Chem.* **2011**, *21*, 10641.
9. Bao, H.; Yang, J.; Huang, Y.; Xu, Z. P.; Hao, N.; Wu, Z.; Lu, G. Q.; Zhao, D.; *Nanoscale* **2011**, *3*, 4069.
10. Harrison, R.; Li, L.; Gu, Z.; Xu, Z. P.; *Microporous Mesoporous Mater.* **2017**, *238*, 97.
11. Cao, W.; Muhammad, F.; Cheng, Y.; Zhou, M.; Wang, Q.; Lou, Z.; Li, Z.; Wei, H.; *ACS Appl. Bio Mater.* **2018**, *1*, 928.
12. Meynen, V.; Cool, P.; Vansant, E. F.; *Microporous Mesoporous Mater.* **2009**, *125*, 170.
13. Le Bail, A.; Duroy, H.; Fourquet, J. L.; *Mater. Res. Bull.* **1988**, *23*, 447.
14. Rodríguez-Carvajal, J.; *Phys. B* **1993**, *192*, 55.
15. Grün, M.; Unger, K. K.; Matsumoto, A.; Tsutsumi, K.; *Microporous Mesoporous Mater.* **1999**, *27*, 207.
16. Magri, V. R.; Duarte, A.; Perotti, G. F.; Constantino, V. R. L.; *ChemEngineering* **2019**, *3*, 55.
17. Chibwe, K.; Jones, W.; *J. Chem. Soc., Chem. Commun.* **1989**, 926.
18. Mascolo, G.; Mascolo, M. C.; *Microporous Mesoporous Mater.* **2015**, *214*, 246.
19. Troutier-Thuilliez, A.-L.; Taviot-Guého, C.; Cellier, J.; Hintze-Bruening, H.; Leroux, F.; *Prog. Org. Coat.* **2009**, *64*, 182.
20. Demoisson, F.; Piolet, R.; Bernard, F.; *Cryst. Growth Des.* **2014**, *14*, 5388.
21. Thommes, M.; Kaneko, K.; Neimark, A. V.; Olivier, J. P.; Rodriguez-Reinoso, F.; Rouquerol, J.; Sing, K. S. W.; *Pure Appl. Chem.* **2015**, *87*, 1051.
22. Hudec, P.; Smiešková, A.; Jorík, V.; *Stud. Surf. Sci. Catal.* **2008**, *174*, 981.

Submitted: October 24, 2021
Published online: March 8, 2022